

Volution's Evolution

Carlo H. Séquin

EECS, CS Division, University of California
Berkeley, CA 94720-1776, U.S.A.
E-mail: sequin@cs.berkeley.edu

Abstract

“Volution” refers to a series of shell-like modular sculptural elements embedded in a cube. They all have similar edge-patterns consisting of quarter-circles on faces of the unit cube, and on the inside they exhibit several, possibly warped, saddles and tunnels. This paper discusses the origin of these designs and their evolution and development into constrained minimal surfaces and into potentially large-scale, freestanding sculptures.

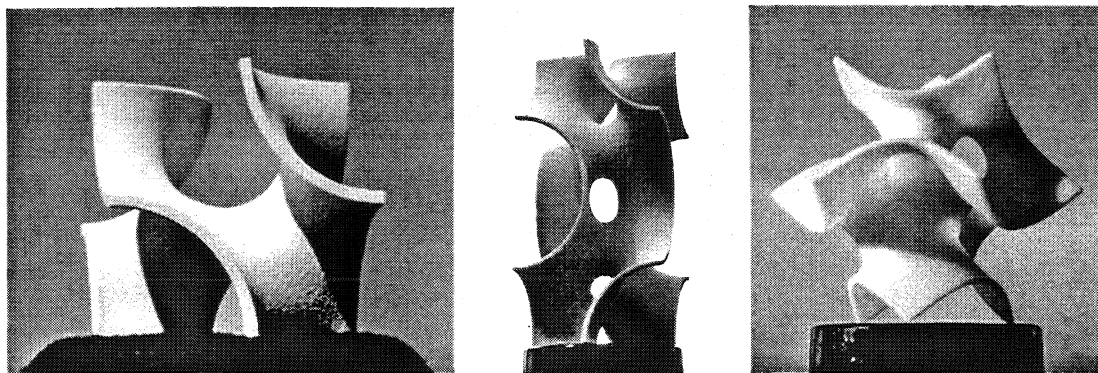


Figure 1. (a) *Volution_0*, (b) stack of two mirrored *Volution_1*, (c) *Volution_5*.

1. Introduction

Webster’s Dictionary defines *volution* as: 1) a spiral turn or twist, 2) a whirl of a spiral shell.

Here, *Volution* is used as the name for a family of constrained minimal surfaces embedded in a cube, exhibiting several possibly warped saddles and tunnels (Fig.1). On each of the six cube faces, the edges of these surfaces exhibit two quarter-circles around opposite corners with radii equal to half the edge length of the cube. Depending on the mutual orientation of this pattern on the six cube faces, different overall edge patterns will result. Originally my attention was focused on the case where all twelve quarter-circles form a single, closed, asymmetrical cycle that forces the spanning surface to form two twisted interlocking valleys with a single strongly warped saddle at the center. The development of this surface has many roots, which will be discussed in Section 2. A systematic taxonomy of the various other edge-patterns is attempted in Section 3. Subsequent sections demonstrate the evolution of spanning surfaces embedded in these edge cycles, from simple warped disks to higher-genus forms, as multiple tunnels and additional saddles are added between the flanges of the disk. Finally, the problems associated with stacking such *Volution* modules in one or more directions are discussed, as well as the constraints on the surfaces to make this possible with G^1 (tangent-) or G^2 (curvature-) continuity, so that these surfaces can be turned into modular sculptural or architectural elements.

2. Background

The *Volution* forms embedded in these curvy edge-patterns in a cube have many independent conceptual roots, and there were several stimulating events that led to the study of these shapes.

The *Iggle*

In Fall of 1999, when I visited NC State University, I was shown a design by Professor Percy Hooper in the Industrial Engineering Department for a modular cubical brick, locally referred to as the *Iggle* (Fig.2). This model had six pairs of quarter-circle flanges on the faces of a cube, and the space between them was modeled with some smooth surface patches. I was given a boundary representation of this shape in STL format and used our FDM machine [16] to fabricate a physical model. Since the curved patches were not joined with tangent continuity, some ridges are apparent on the saddle surfaces. With this object in hand, I started to wonder, how one could model a surface with completely smooth valleys, and what an infinitely thin surface would look like connecting similar quarter-circle arches on a cube surface.

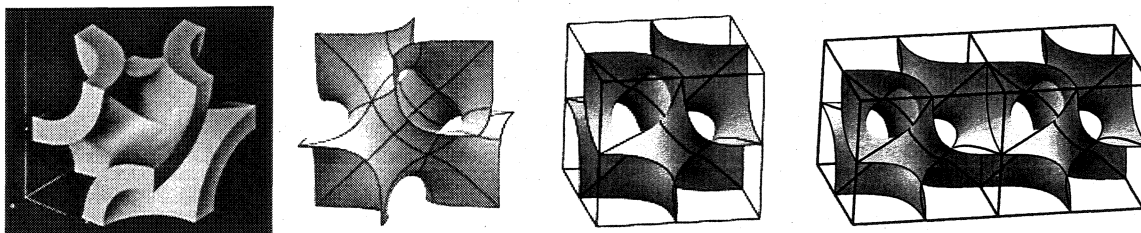


Figure 2. (a) *Iggle* part designed by Percy Hooper [6], (b) Schoen's *F-RD Surface*, (c) Schoen's *Batwing Surface*, (d) two of Brakke's *Pseudo-Batwing modules*[2].

Triply Periodic Minimal Surfaces

A web page by Ken Brakke [2] describes several triply-periodic minimal surfaces. A few among them also have edge patterns consisting of more or less circular arcs on the faces of a cube. However, the pairs of arcs on the cube faces are oriented differently from the boundary of the *Iggle*, leading to different connectivity between the individual edges – and typically to more symmetrical structures.

In particular, *Schoen's F-RD Surface* is a unit cell with tetrahedral symmetry (Fig.2b). It may be viewed as a central chamber from which tubes extend to four alternating (tetrahedral) corners of the cube. This is actually only one eighth of a complete lattice cell with translatory symmetry; the complete cell is obtained by mirroring this sub-cell on its faces. Also, the edges are not strictly circular, when the surface area is minimized in the larger lattice cell. However, this cube-like base domain would still make a nice modular building element.

Another related element is the *Batwing Surface*. It was given this name, because of the peculiar shape of the fundamental regions shown outlined on the surface in Figure 2c. Twenty-four of those regions make the complete cuboid element shown. Again, this is only 1/8 of the complete minimal surface lattice cell. Brakke then assembled two of these cells in a different way, using a C_2 symmetry operation with axes along the face diagonals of the cube. This produces a slightly different geometry for the fundamental region, which he calls *Pseudo Batwing Surface* (Fig.2d).

In *Schoen's F-RD Surface* (Fig.2b) the twelve quarter-arcs form four closed circuits around four alternating corners of the cube. In the *Batwing* elements, the twelve edges are connected into a single closed circuit. This is also true for the *Iggle*, but the actual connectivity, and thus the symmetry of the overall object is different. *Batwing* has cyclic C_3 -symmetry around one space diagonal of the cube,

whereas *Iggle* has D_2 symmetry, comprising three mutually perpendicular C_2 rotation axes. It is natural to ask, what the genus-0 minimal surfaces within these two edge patterns would look like, if the edge patterns were forced to be comprised of exact quarter circles; this is known as Plateau's problem [11].

Stewart's Surface

In March 2001, Jeff Hrdlicka [7] sent me pictures of an intriguing surface created by P. J. Stewart (Fig.3a). Starting from three mutually perpendicular circles, forming the wire frame of a spherical octahedron, Mrs. Stewart used wire-mesh loops to build ribbons following an Eulerian edge path that covers every edge once and touches every vertex exactly twice. She then created further wire loops to broaden that ribbon along the edge cycle and continued until the surface smoothly connected in the center of the octahedron (Fig.3a). To understand the pictures received, I emulated this process in a wire frame of a polyhedral octahedron, filling in the surface with scotch tape. It is fascinating to see, how the ribbons join naturally in the middle, and how the logic of the surface emerges without ambiguity. I then emulated that shape with a subdivision surface and produced an FDM maquette (Fig.3b). Once I had the physical model in hand, the central part of the surface looked oddly familiar.

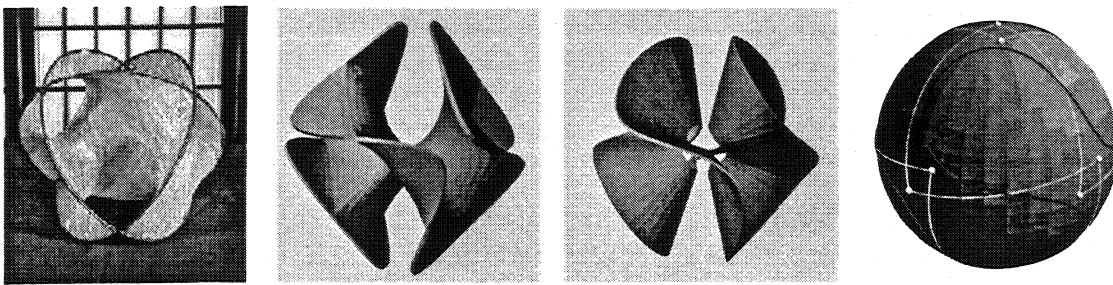


Figure 3. (a) P.J. Stewart's Surface, (b) FDM surface in Octahedron, (c) Aurora sculpture, (d) Aurora's sweep path on the sphere.

Aurora

In the winter of 2000, I had worked on the *Viae Globi* series [14], a study of sculptural models based on various loopy curves on the surface of a sphere. This work was inspired by Brent Collins' *Pax Mundi* [3] and thus mostly featured narrow, channel-like, swept paths along such spherical splines. However, in other instances, I also had used just flat, ribbon-like cross sections. In one sculpture, called *Aurora* (Fig.3c) I had oriented that ribbon in such a way that one of its edges always pointed toward the center of the sphere; that ribbon resembled the curtain-folds that one occasionally sees in an aurora borealis. In some preliminary studies, I had extended that ribbon fairly close towards the sphere center and wondered how I might smoothly close the resulting rugged hole. With copious use of scotch tape, I was able to form a highly twisted saddle to do the job.

A Common Theme

When I later compared the sweep path for *Aurora* with the edge pattern of *Stewart's surface*, it turned out that *Aurora's* spline path was simply a smoothed version of the Eulerian path on the octahedron. The defining sweep curve of *Aurora* used a cubic B-spline on a sphere with twelve control points that lay on a path very similar to that of a spherical octahedron (Fig.3d). Suspecting further, that the *Iggle* surface was also a close relative, I later found that a central projection of its edge pattern onto a sphere also produced a very similar curve. All of the rim shapes of *Iggle*, *Stewart's surface*, and *Aurora*, are topologically equivalent to a simple circle, and thus their interiors can be spanned by some warped disk, which at the center exhibits the shape of a helically twisted biped saddle. This shape can also be understood as a progression of individual biped saddles that form a warped canyon.

3. Charting All Possible Edge Cycles

Rotating the edge patterns on some of the cube faces by 90° will lead to differently interconnected edge cycles. We have seen two patterns that connect all twelve arcs into a single edge-cycle. How many different such patterns are there? What kinds of (minimal?) surfaces can be embedded in them? And which ones of them do have aesthetic merits as a sculpture? We start the systematic exploration of all such *Volusion* surfaces by first constructing all possible edge patterns.

Keeping one cube face fixed and rotating some of the others individually by 90° , leads to 32 different configurations that must be examined. One can quickly see that many of them are equivalent. To classify all possible configurations, we start by counting the number of individual edge cycles in each pattern; among those we can then easily distinguish eight different geometrical constellations (Table 1). These patterns are illustrated in Figure 4 on the unfolded nets of the bounding cubes.

Table 1: The different edge cycle patterns

"4"	1 instance	4 ears in tetrahedral configuration	Fig.6a
"3b"	2 instances	3-fold symmetrical Costa surface	Fig.6c
"3a"	6 instances	1 trench plus 2 ears	Fig.6b
"2b"	3 instances	2 trenches = Mace configuration	Fig.5b
"2a"	12 instances	C-valley plus a single ear	Fig.6d
"1c"	2 instances	3-fold symmetrical Gabo curve	Fig.2c
"1a,b"	6 instances	Left- and right-handed Iggle curves	Fig.1a

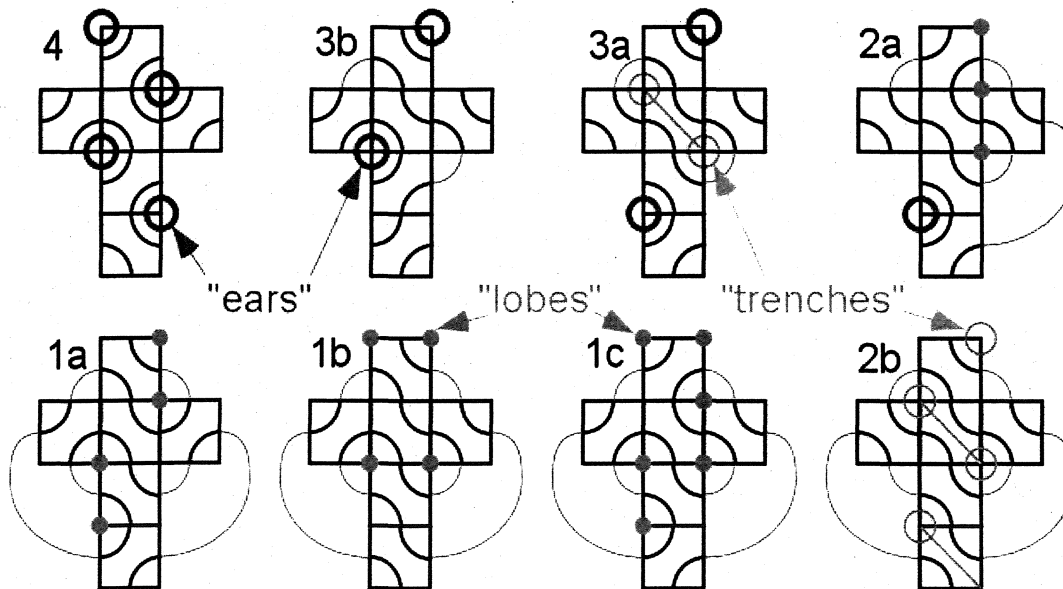


Figure 4. Eight generic edge configurations out of 32 possible ones.

Edge cycles can be of length 3, 6, 9, and 12 quarter-circles. Cycles of length 3 form "ears" around a single corner of the cube. Length-6 cycles either connect two adjacent ears into a "trench", or they form a wavy equatorial "belt". The cycle of length 9 forms a "C-shaped" valley; and the full-length, 12-edge

cycle can either separate two warped Z-shaped valleys as in the *Iggle*, or it can form an oscillating, 3-period Gabo curve [14] around the equator as in the *Batwing* modules. In summary, only the eight combinations shown in Table 1 can occur under all possible orientations of the cube faces. In the following, we will discuss these basic edge patterns and illustrate them with suitable spanning surfaces.

4. Simple Spanning Surfaces

Volution shells are all spanning surfaces in one of the above boundary component patterns. In general there exist several different spanning surfaces for each pattern. We will start by describing the simplest surfaces that do not reduce the symmetry group defined by the given edge pattern.

For a single-cycle edge pattern, the simplest surface has the topology of a disk, i.e. is of genus 0. Such a surface can be constructed by connecting all points on the edge cycle with straight line-segments to the center of the cube, and then “relaxing” this surface into a minimal surface in the Surface Evolver [1]. For cases “1a” and “1b” we obtain the basic genus-0 *Volution* shell (Fig.1a). For case “1c”, resembling a third-order Gabo curve [14], a 3-fold symmetrical monkey-saddle is formed at the cube center (Fig.8a).

A spanning surface between multiple boundary components may correspond to an annulus or a disk with multiple holes (all still genus 0). For our edge patterns, the resulting 3D shapes typically exhibit some tunnels, and it is somewhat tricky to figure out how many of them correspond to topological handles that will add to the genus of the surface. With only two boundary components, as in pattern “2b”, the simplest surface may look like a buckled cylinder (Fig.5a), which could then be smoothed into a shape resembling a piece of a single-shell hyperboloid (Fig.5b).

However, since valleys formed by edge cycles comprising more than 3 quarter-circles yield two or more “lobes” near the corners of the cube which are separated by narrower “gorges” near the face centers, it is more “natural” (emulating the shape of a soap film) to terminate any tunnels in the centers of these lobes, rather than in the middle of a constriction. Maintaining the symmetry defined by the edge pattern, will add further constraints; e.g., for the case “2b”, the two trenches should be connected either by four tubes placed along space half-diagonals of the cube, leading to a central cavity; this forms a surface of genus 2 (Fig.5c). Alternatively, we could run four tubes parallel to the face diagonals of the cube, resulting in a genus-3 surface (Fig.5d).

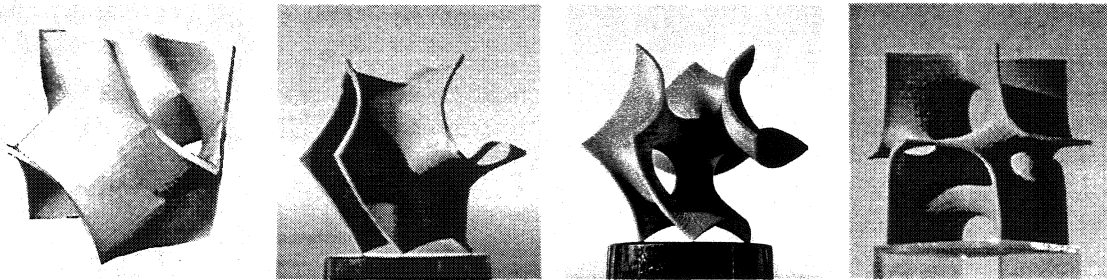


Figure 5. Three different spanning surfaces for edge pattern “2b”: (a,b) genus 0 (SLIDE simulation & FDM model), (c) genus 2 (subdivision surface), (d) genus 3 (minimal surface).

The maximum number of edge cycles that can occur is four. There is only one such pattern “4”, and it exhibits tetrahedral symmetry. We can readily fit a genus-0 surface of the type shown in Figure 2b into this pattern using space-diagonal tubes (Fig.6a). Alternatively the four ears could be connected in pairs by six tubes following the edges of a tetrahedron, creating a genus-3 surface without loss in symmetry.

By rotating a single cube face, two of the four “ears” are connected into an elongated “trench” and a 3-cycle pattern results; there are six occurrences of this pattern “3a” in the complete survey. In Figure 6b we have used 5 face-diagonal tubes to connect the two ears (top) to the trench (bottom) and to each other.

This also forms four space-diagonal openings between the ears and the trench, which lead to a central chamber. This is a surface of genus 3.

For the case “3b” the two 3-edge ears are on different sides of the larger, equatorial cycle formed by 6 quarter-circles. This configuration has D_{3d} symmetry just like the Gabo-3 configuration. However, it has the basic edge configuration of a Costa surface [5]; thus it seems natural to try to embed such a surface into this cubical cell. Because of the inherent C_3 symmetry of the edge pattern, it is natural to chose a genus-2 Costa surface [5], where the two funnels coming in from either end split into three tunnels each (Fig.6c).

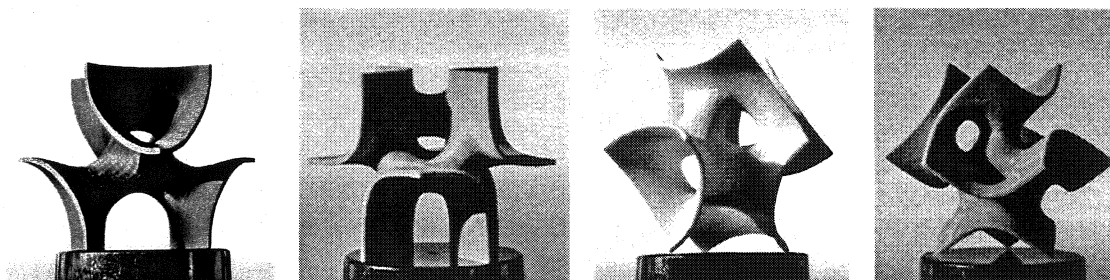


Figure 6. Spanning surfaces in various edge patterns: (a) “4”, (b) “3a”, (c) “3b”, (d) “2a”.

Twisting a second face of shape “3a” can either elongate this trench into a C-shaped canyon, i.e. pattern “2a” (Fig.6d), or it can connect the remaining two ears to form a configuration with two trenches at a 90° angle from each other, i.e. pattern “2b”, reminiscent of the structure of Charles O. Perry's *Mace* sculptures [10]. Figure 6d shows a surface of genus 3. Three surfaces of different genus that can be embedded in this *Mace* configuration have already been discussed above (Fig.5).

While the tunnels in the Costa surface (Fig.6c) naturally fall into place, the other 2- and 3-cycle edge patterns offer less obvious choices concerning the topology of their spanning surfaces. The edge patterns most commonly occurring in the survey, “2a” and “3a”, exhibit one or two isolated ears combined with a longer edge cycle. For these 2- and 3-cycle structures, we can readily add face- or space-diagonal tubes to connect all ears and trenches so as to form a connected surface. For case “2a” (Fig.6d) I have used four face-diagonal tubes surrounding a central tetrahedral chamber. For these less symmetrical edge patterns, we also have to choose, whether we want to form an additional saddle (of potentially higher order) at the center of the cube. Since these shapes have lower symmetry and appear to have less aesthetic appeal, I have not pursued them thoroughly, so far.

Among the single-cycle patterns, we only find the two patterns that we are already familiar with: the *Iggle* pattern and the *Gabo-3* pattern. It can be seen that the *Iggle* pattern, and thus all the basic *Volution* shells, come in two versions, “1a” and “1b”, which are mirror images of each other.

5. Additional Tunnels

Tunnels clearly make these structures interesting. We can also try to enhance the simple warped-disk forms by adding tunnels between pairs of suitable chosen flanges. As a general rule, since all of these surfaces are two-sided, and thus could be painted with two different colors, the entry and exit openings of a tunnel must lie in regions of the same color.

For edge pattern “1c” we have already seen a spanning surface with “naturally occurring” tunnels in the *Batwing* modules (Fig.2c). Each “lobe”, defined by two contiguous quarter circle arcs turning around the same cube corner, forms an entrance to a tunnel. These six openings are connected into two stacked Y-configurations of tunnel junctions that lie above and below a central monkey saddle.

In a similar way, we can enhance the basic *Iggle* configuration. The *Volution_0* surface has four “lobes” which form the ends of the two tortuous Z-shaped canyons on either side of the central saddle. The inner parts of two of these lobes are red and two are blue, if the original disk is painted with these two colors on its two sides. Adding two separate tubes, connecting the two pairs of entrances with matching colors, while maintaining the given D_2 symmetry, leads to *Volution_2* (Fig.7a), a surface of genus-2 that resembles an irregularly twisted 5-story Scherk tower [13].

There is a simple and graceful way to increase the genus by only 1 without destroying the D_2 symmetry. As in the case of the *Batwing* module, we can push the two tunnels close to the center of the cube, so that they touch and form a saddle between them. This results in a simpler structure of genus 1 (Fig.7b). We can further increase the genus of these *Volution* shells by adding face-diagonal tubes between any two flanges ending in the same cube surface. Adding four such tubes to *Volution_1* along the side faces of the cube, results in a very intriguing surface of genus of 5 (Fig.7c). On the other hand, doing the same thing with *Volution_2*, leads to a structure that becomes too cluttered.

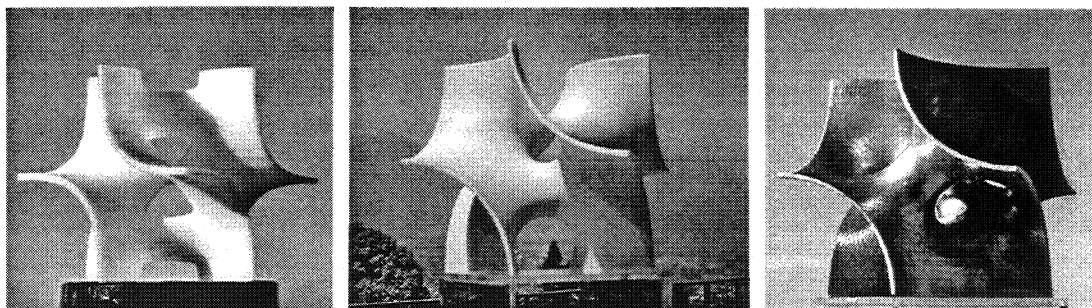


Figure 7. (a) *Volution_2*, (b) *Volution_1*, (c) *Volution_5*.

These exploratory models were realized quickly as plastic maquettes built on an FDM [16] rapid prototyping machine. Using the SLIDE environment [15], I first designed thin polyhedral 2-manifolds of the proper topology and with the maximal symmetry possible. These models had from 30 to 60 facets, and were provided with 2 to 4 continuously adjustable numerical parameters that define the position of some of the key vertices in these polyhedral models. By moving these vertices, the diameter of the tunnels and their distances from the cube center, or the extension and curvature of the flanges can be adjusted interactively. I then used SLIDE's *subdivision* module to send these manifolds through three generations of Catmull-Clark surface refinements. The twelve outer corners located at the edge centers of the basic cubic cell were flagged to keep their original positions while undergoing this approximating subdivision procedure – otherwise the edges would have been rounded to something like an *Aurora*-like rim shape (Fig.3c). Once I had adjusted the shape parameters to end up with a satisfactory subdivision surface, I used SLIDE's *offset-surface* module to turn the thin manifold into a surface slab of sufficient thickness, so that it could be built with a layered-manufacturing rapid-prototyping process. These physical maquettes were very important in comparing the various topologies and in selecting the shapes that seemed worthwhile to be optimized for aesthetic criteria and/or to be turned into true minimal surfaces.

6. Constrained Minimal Surfaces

For the promising, not-too-cluttered geometries, I wanted to explore, whether these manifolds can be turned into true minimal surfaces – and perhaps into periodic building blocks. For a few of the edge configurations, i.e. for the tetrahedral 4-ear configuration and for the Gabo-3 curve, the answers can be seen on Brakke's webpage [2]. For the latter edge configuration, we can also omit the tunnels and then obtain the classical monkey saddle (Fig.8a). Other configurations require additional studies. Fortunately, once we have an initial polyhedral mesh that defines the topology of an interesting shape, we can readily

send it through the Surface Evolver [1] and try to obtain a true minimal surface. If we start with the 3-cycle edge configuration that affords the topology of a genus-2 Costa surface, the Surface Evolver, reveals that this particular edge configuration embedded in the surface of a cube indeed allows the formation of a true, albeit unstable minimal surface. The result is a very attractive sculpture (Fig.8b).

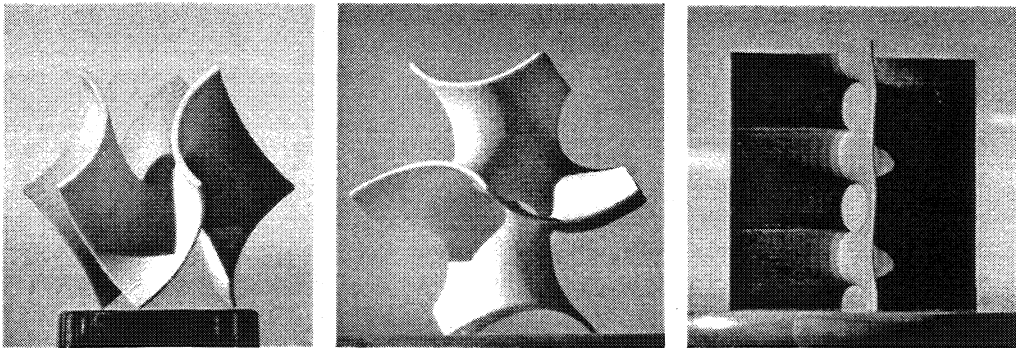


Figure 8. Classical minimal surfaces: (a) Monkey saddle, (b) Costa surface, (c) Scherk's surface.

Volution_0, *Volution_1*, and *Volution_5* also looked attractive enough so that it was worthwhile to study the minimal surfaces that they might generate. *Volution_0* presented no problem (Fig.9a). The central point was fixed in the middle of the cube, in accordance of the inherent symmetry of this shape. This symmetry, captured in the polyhedral description, was maintained during the relaxation process in the Surface Evolver. However, an actual physical soap film would not remain in this unstable equilibrium.

On the other hand, *Volution_1* has asymmetrical saddles between each of the central tunnels and the outer "half-tunnels" between the pairs of edges in the top and bottom faces of the cube. If this saddle is not perfectly balanced, it will move in the direction of the narrower tunnel. For the standard quarter circles on the top and bottom cube faces, the inner-tunnel has more contraction power and will collapse, if the Surface Evolver is run long enough. However, this process is slow enough, so that we can capture a pleasing state for a stand-alone sculpture; but we should be aware, that this is not a true minimal surface but only a snapshot in a run-away process. Only by changing the quarter circles on the top and bottom faces into hyper-quadrics, so that they can approach each other more closely, one can make sure that the outer half-tunnel has a strong enough contraction force, so that we can find an initial balance point that will lead to an (unstable) equilibrium configuration of the final surface shape.

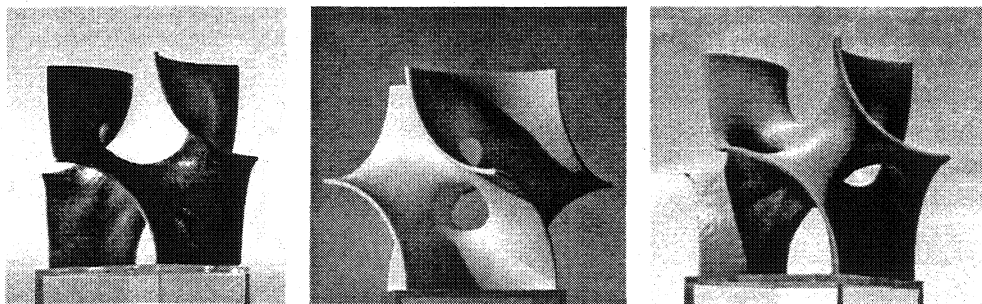


Figure 9. (a) Unstable "minimal" surface of genus 0, (b,c) snapshots of a run-away minimization process for surfaces of genus 1 and 5, respectively.

As we add more tunnels, more instabilities arise. In *Volution_5* we have two types of "inner" tunnels that need to be balanced against their adjacent outer half-tunnels – as well as against each other! Again, we can readily capture a pleasant state of the evolving surface before any tunnel collapses (Fig.9c).

Adjacent tunnels forming saddles between them is not something one typically sees in nature, but mathematical illustrations of minimal surfaces are full of such configurations. Even the basic Scherk minimal surface (Fig.8c) is unstable and would end up in run-away disaster, if one of the holes got slightly larger or smaller. In more complex structures, the point of balance between any pair of such tunnels has to be found by a binary search for the proper initial position of the shared wall between them. For structures with n different kinds of tunnels, there may be as many as $n(n-1)/2$ shared walls that need to be adjusted, and the balancing process can become quite tedious.

7. Modular Building Blocks

Since we have confined the edges of all these surfaces to the same standard quarter-circles on all the cube faces, these elements can readily be stacked together in all three directions and have their flanges join without gaps (Fig.10). However, there is no guarantee that these flanges will join with tangent continuity. If we look more closely at some of the stacking examples, we can indeed see such discontinuities. To avoid such discontinuities one can send two abutting modules jointly through the surface minimization process (Fig.11).

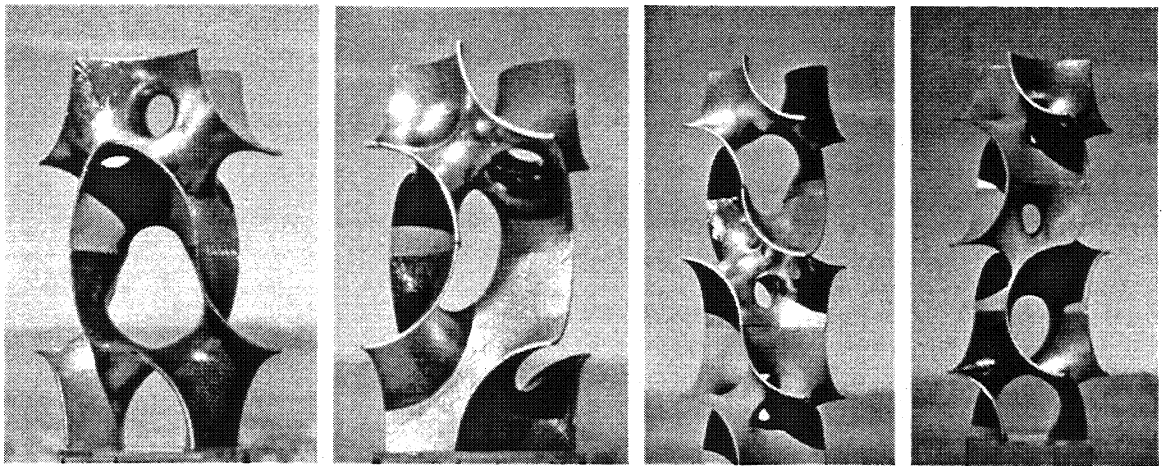


Figure 10. *Stacked modular Volution elements.*

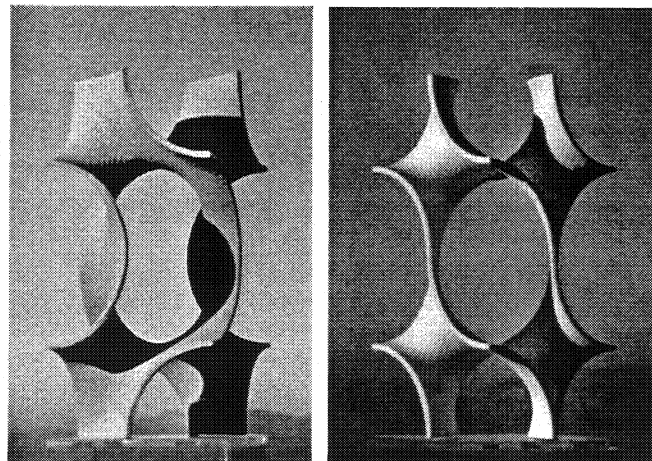


Figure 11. *Minimal surfaces of two joined Volution_0 elements: (a) mirrored, (b) C_2 -rotation.*

To guarantee tangent continuity at these seams, one could demand that the surfaces terminate perpendicularly on the cube surfaces. This condition can be achieved by specifying the cube surfaces to act like “mirrors” in the Surface Evolver. This has the same effect as evolving a pair of joined modules together with a loose boundary between them (Fig.11). However, this means that we can no longer specify the shape of the boundary curve, and the resulting curves will be different when we combine different modules in different ways. In general, the edges will then no longer be quarter-circles! In particular, when two cells are joined with C_2 symmetry, the shared edge becomes a straight line (Fig.11b). Thus the resulting *Volution* elements can then only be stacked using equivalent cube faces, but not by joining arbitrary sides.

To obtain a totally modular element that can be stacked on all six cube faces with arbitrary combinations of the orientations of adjoining modules, several conditions have to be fulfilled:

1. To guarantee G_0 (surface-) continuity, the boundaries must be of a fixed, predefined shape, i.e., they must all be exact quarter circles.
2. To guarantee G_1 (tangent-) continuity along all possible seams, the surface must meet the cube faces perpendicularly along all its boundaries.
3. To guarantee G_2 (curvature-) continuity, the curvature perpendicular to all the boundaries must be a predefined constant, i.e., zero.

Condition 1.) can be fulfilled by a minimal surface – and that is what we have done with our *Volution* elements discussed above. If we also want to fulfill condition 2.), we need an energy functional of higher order. Brakke’s Surface Evolver also provides code for the Willmore energy functional [8], which minimizes bending energy, i.e. the area integral over the square of curvature. This functional allows us to specify position as well as surface normal along the boundary curves. With those constraints we could create modular blocks that exhibit G^1 continuity across their seams when put together.

In order to accommodate all three requirements simultaneously, we need an optimization function of even higher order. A possible candidate is the MVS functional, which minimizes the area integral of the derivative of curvature [8]. This functional seems to optimize surface aesthetics in many different situations [12]. However, we are not aware of a robust and efficient implementation of this functional. The multiple nested optimization loops of the original demonstration code, used to maintain C^1 and C^2 continuity between all the bi-quintic Bézier patches, are far too slow. A different internal representation that automatically maintains continuity through its underlying construction, e.g., through the use of a subdivision surface, could remedy this problem.

Figure 12 shows stacking examples using *Volution_1* minimal surface elements.

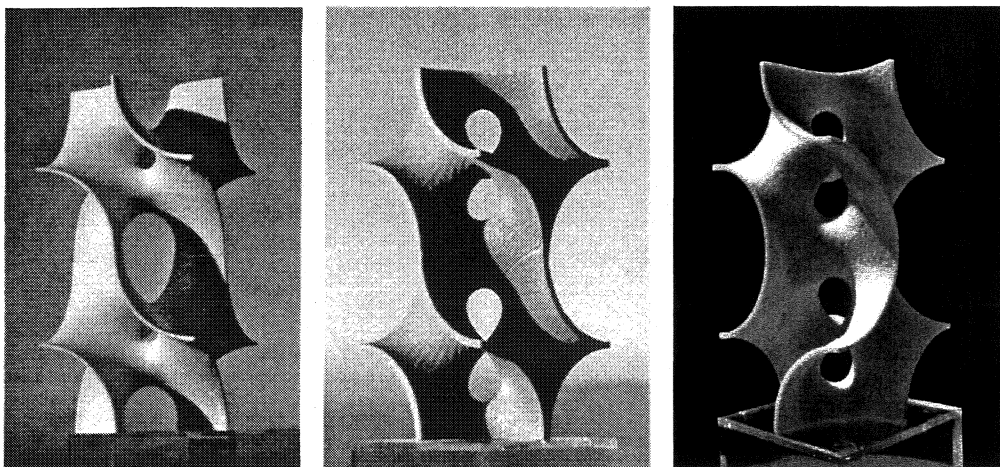


Figure 12. Two *Volution-1* elements: (a) stacked, (b,c) jointly evolved to minimal surface.

8. Minimality and Aesthetics

The evolution surfaces emerging from the Surface Evolver look beautifully balanced, and there is no obvious way in which these shapes could be aesthetically improved. Does this mean that minimal surfaces represent an aesthetic optimum in general? A few experiments give some insight into this question.

In one experiment, John Sullivan has approximated the edge curve of *Atomic Flower 2* [4] sculpted by Brent Collins with smooth mathematical curves that result in the same symmetry, and then used Brakke's Surface Evolver to minimize a suitable spanning surface [17]. I thickened this minimal surface by computing an offset surface in SLIDE [15], and then fabricated a maquette on our FDM machine (Fig.13a). When comparing this model to the original sculpture, it becomes clear that Collins' original artwork has superior aesthetics. A key difference is visible in the narrow looping ribbons. The original ribbons have a strong lateral curvature to make them into distinct channels that evoke physical strength and stability, and which turn them into interesting 3-dimensional elements. The true minimal surface, on the other hand, needs to balance the lateral curvature with the curvature in the longitudinal direction. This makes these ribbons almost flat, and clearly less visually interesting.

A second experiment involved the *Minimal Saddle Trefoil* which resulted from the early phases of my collaboration with Brent Collins. In this case, the best-fitting (4,3) torus knot was used as the constraining edge curve for a minimal surface, and again a maquette was made (Fig.13b) for direct comparison with my original design coming out of my *Sculpture Generator I* [13]. In this case, I prefer the shape produced by the Surface Evolver. The differences are subtle and mostly related to the exact shape of the edge curve. Specifying a perfect torus knot curve avoids some of the unnecessary undulations produced by my ad hoc representation in the *Sculpture Generator I*, which is based on a sequence of stacked hyperbolas.

As a third experiment we have taken the edge constraints of the spherical octahedron and embedded an approximation of Stewart's surface in it. The Surface Evolver then turned this into the minimal surface shown in Figure 13c – a very pleasing, well-balanced shape.

What can we conclude from these experiments? It seems that for large surfaces, deviations from minimality do not produce any aesthetic gains. However, if the sculpture involves narrow, ribbon-like parts, artistic freedom can produce aesthetic gains over the perfect minimal surface geometry. In the case of the *Volution* shells, the surfaces are wide enough, so that we can readily use the true minimal surface as the aesthetic optimum.

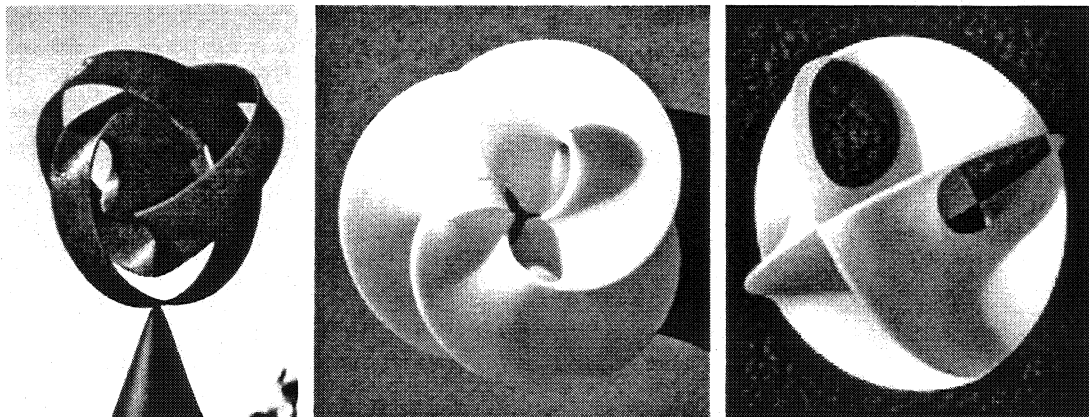


Figure 13. Reconstructions as true minimal surfaces: (a) Collins' *Atomic Flower 2*, (b) Séquin's *Minimal Saddle Trefoil*, (c) Stewart's *spanning surface in a spherical octahedron*.

9. Conclusions

The detailed investigation of a warped saddle surface embedded in a predefined edge structure has led to the discovery of fascinating connections between constrained minimal surfaces, modular architectural building blocks, and triply periodic minimal surfaces. It has also resulted in the discovery of several aesthetically very attractive shapes, which can either stand on their own as large scale sculptures or which can be combined in a modular manner.

Acknowledgements

The help of Cathy Tao and Trai Le in running some of these models through Brakke's Surface Evolver are greatly appreciated. Many thanks also go to John Sullivan for his thorough review of the paper and for helping me understand how to determine the genus of surfaces with multiple boundary components.

References

- [1] K. Brakke, *Surface Evolver*, – <http://www.susqu.edu/facstaff/b/brakke/evolver/> (2003).
- [2] K. Brakke, *Triply Periodic Minimal Surfaces*, – <http://www.susqu.edu/facstaff/b/brake/evolver/examples/periodic/> (2003).
- [3] B. Collins, *Finding an Integral Equation of Design and Mathematics*, Proc. Bridges'98, Fig.22, p27.
- [4] B. Collins, *Merging Paradigms*, Proc. Bridges'99, Fig: Atomic Flower 2, Appendix. (1999).
- [5] D. A. Hoffman: *Costa Surfaces*, – <http://www.msri.org/publications/sgp/jim/geom/minimal/library/costa/indexd.html> (2003).
- [6] P. Hooper, *Iggle*, – private communication, NC State University, Raleigh, Fall 1999.
- [7] J. Hrdlicka, *Surface by P. J. Stewart*, – private communication, March 2001.
- [8] L. Hsu, R. Kusner, and J. Sullivan, *Minimizing the Squared Mean Curvature Integral for Surfaces in Space Forms*, Experimental Mathematics 1, p191-208 (1991).
- [9] H. P. Moreton and C.H. Séquin, *Functional Optimization for Fair Surface Design*, Proc. ACM SIGGRAPH'92, Chicago, July 1992, and Computer Graphics, Vol 26, No 2, pp 167-176, (1992).
- [10] C. Perry, *Charles O. Perry*, deCesare Design Assoc., Darien CN, "Early Mace" p52, (1987).
- [11] *Plateau's Problem*, – <http://mathworld.wolfram.com/PlateausProblem.html> (2003).
- [12] C. H. Séquin, P. Y. Chang, and H. P. Moreton, *Scale-Invariant Functionals for Smooth Curves and Surfaces*, Proc. 1993 Dagstuhl Seminar on Geometric Modelling, Hans Hagen, ed., Computing Supplement 10, Springer, pp 303-321, July 1995.
- [13] C. H. Séquin, *Virtual Prototyping of Scherk-Collins Saddle Rings*, Leonardo, Vol. 30, No. 2, 1997, pp. 89-96.
- [14] C. H. Séquin, "Viae Globi" – *Pathways on a Sphere*, Mathematics and Design 2001, Geelong, Australia, July 3-5, 2001.
- [15] J. Smith, *SLIDE environment*, – <http://www.cs.berkeley.edu/~ug/slide/docs/slide/spec/> (2003).
- [16] Stratasys Corp., *FDM machine*, – <http://www.stratasys.com/> (2003).
- [17] J. Sullivan, *Minimal Flower 3*, – <http://torus.math.uiuc.edu/jms/Images/Sculp/> (2003).
- [18] ZCorporation, *3D-Printer*, – <http://www.zcorp.com/> (2003).